ELECTRONIC SUPPLEMENTARY INFORMATION

Investigation of cobalt(III)-tpa complexes as potential bioreductively activated carriers for naphthoquinone-based drugs

Aline Farias Moreira da Silva[a], Renata de Uzeda Vital[a], Daniela de Luna Martins[a], David Rodrigues da Rocha[a], Glaucio Braga Ferreira[a], Jackson Antônio Lamounier Camargos Resende[b], Mauricio Lanznaster[*a]

[a] Instituto de Química, Universidade Federal Fluminense, Outeiro S. João Batista S/N, 24020-141, Niterói, RJ, Brazil

[b] Instituto de Ciências Exatas e da Terra, Centro Universitário do Araguaia, Universidade Federal do Mato Grosso, 78600-000, Barra do Garças, MT, Brazil.

Table S1. Comparison between calculated and experimental bond distances (Å) and angles (º) of $[Co(TPA)(NQ\text{-}CH_3)]^{2+}$ and $[Co(TPA)(NQ^1\text{-}Cl)]^+$.

Distance/angle	$[Co(TPA)(NQ\text{-}CH_3)]^{2+}$		$[Co(TPA)(NQ^1\text{-}Cl)]^+$	
	Exp.	Calc.	Exp.	Calc.
Co-O1	1.923	1.921	1.882	1.877
Co-O2	1.888	1.875	1.884	1.863
Co-N1	1.935	1.962	1.944	1.966
Co-N2	1.915	1.918	1.916	1.910
Co-N3	1.922	1.918	1.934	1.921
Co-N4	1.886	1.895	1.920	1.922
O2-Co-O1	84.92	86.02	87.22	89.05
N4-Co-N1	87.68	87.50	86.67	87.13
N4-Co-N3	88.82	90.48	90.29	90.35
N4-Co-N2	92.52	90.48	91.76	90.50
N1-Co-N2	85.36	85.64	85.76	86.16
N1-Co-N3	85.13	85.64	84.91	85.69
O1-Co-N1	92.68	92.69	93.12	90.97
O2-Co-N4	94.70	93.79	92.95	92.83
O1-Co-N3	89.44	89.53	87.67	88.60
O1-Co-N2	89.28	89.53	90.25	90.28

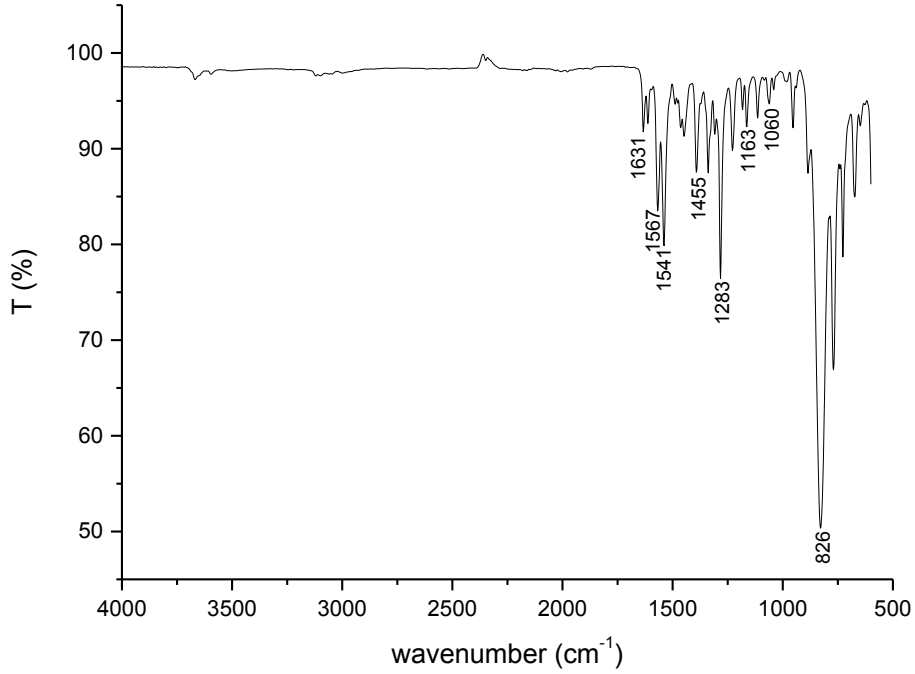

Figure S1. FTIR spectrum (ATR) of **1**.

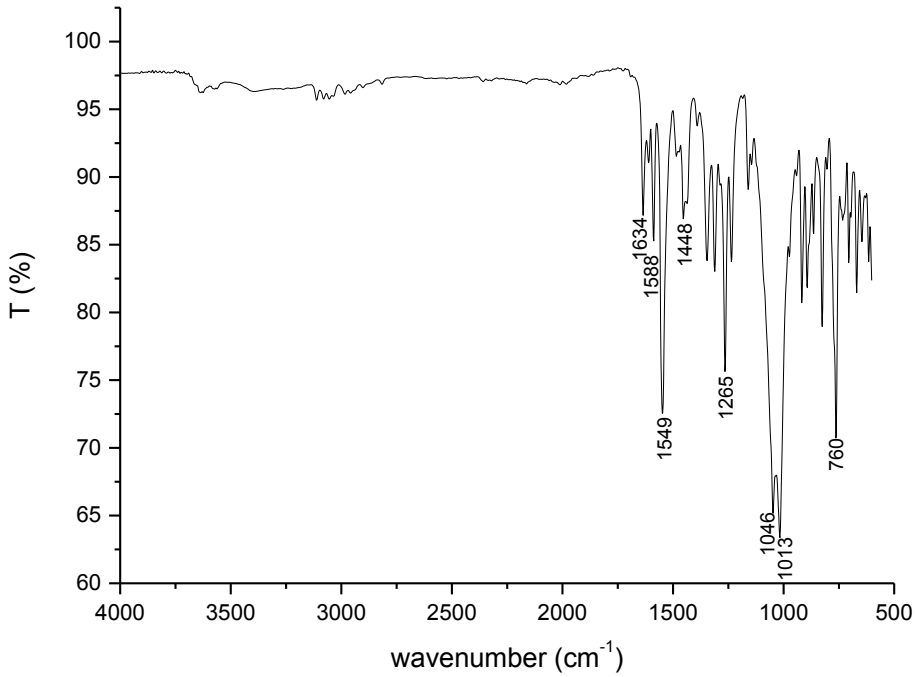

Figure S2. FTIR spectrum (ATR) of **2**.

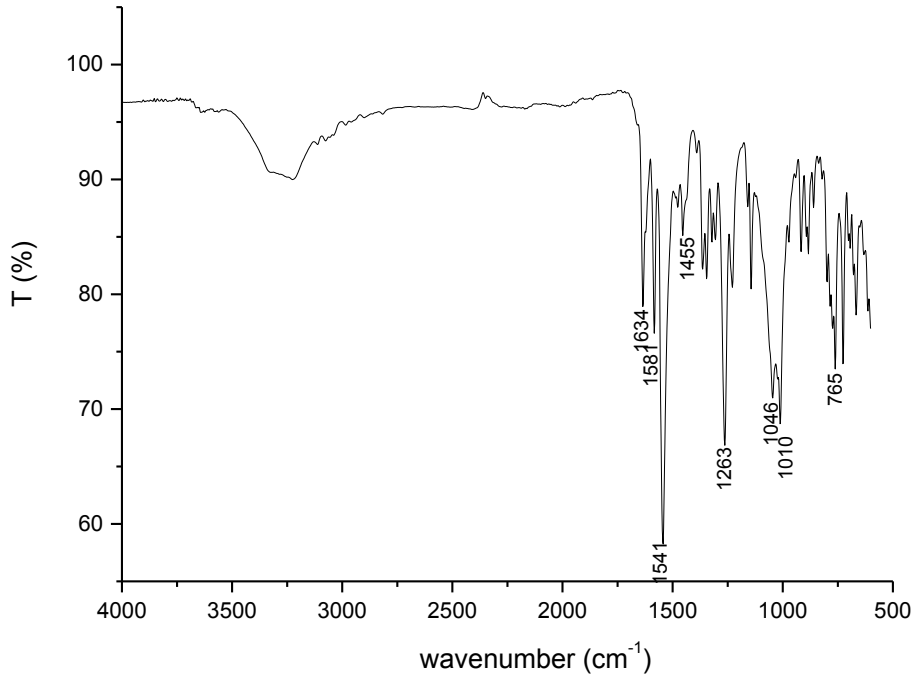

Figure S3. FTIR spectrum (ATR) of **3**.

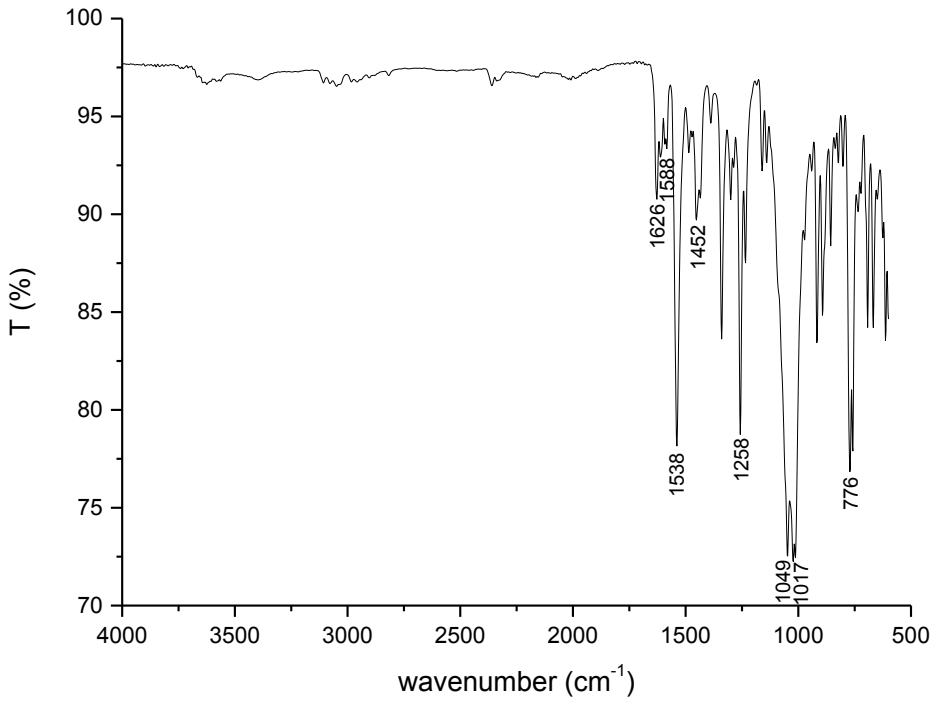

Figure S4. FTIR spectrum (ATR) of **4**.

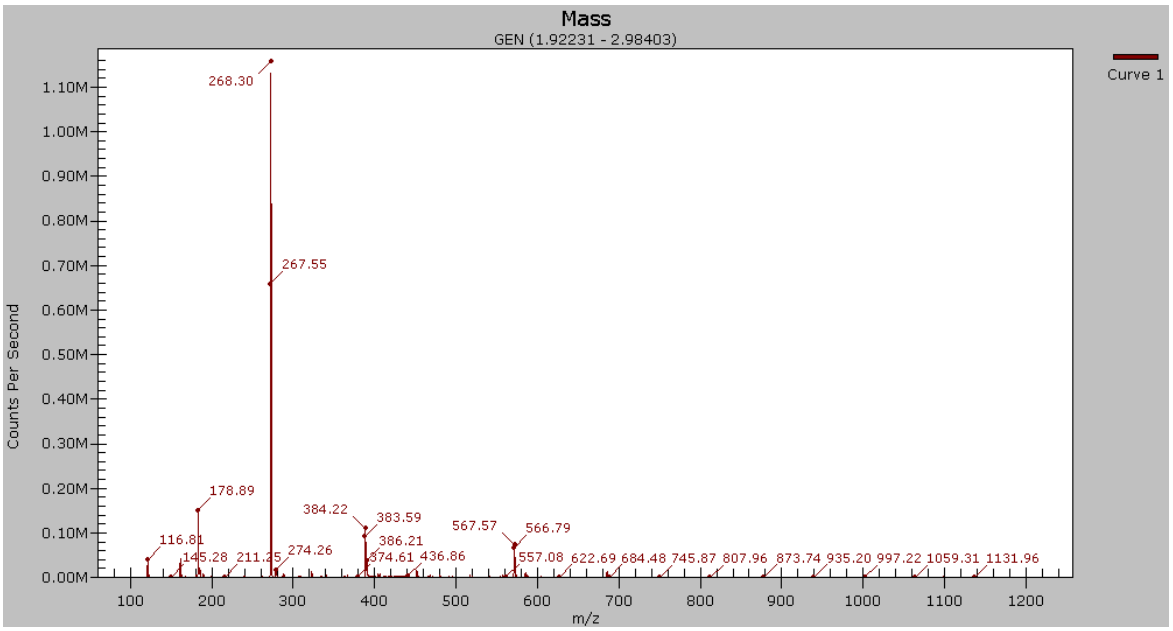

Figure S5. ESI-MS spectrum of **1** in MeCN.

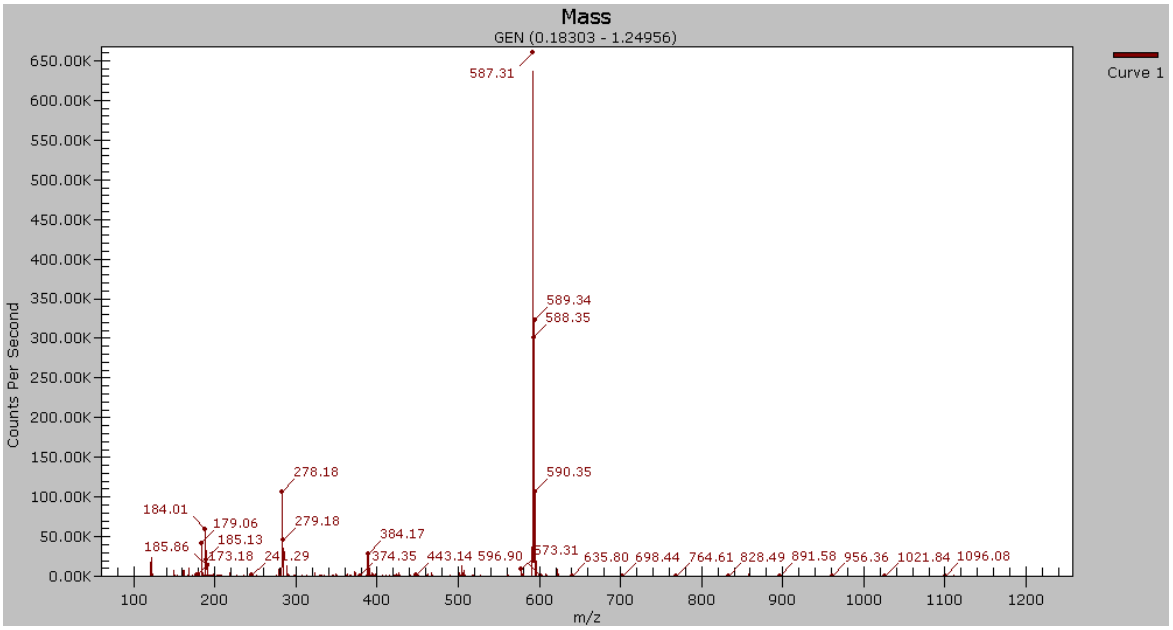

Figure S6. ESI-MS spectrum of **2** in MeCN.

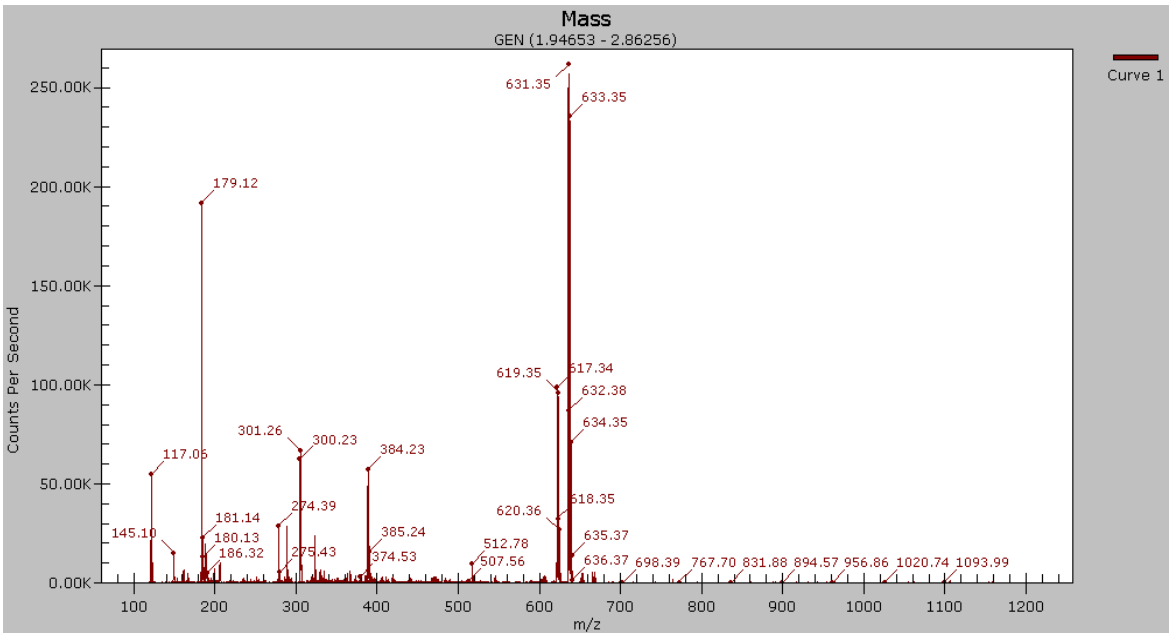

Figure S7. ESI-MS spectrum of **3** in MeCN.

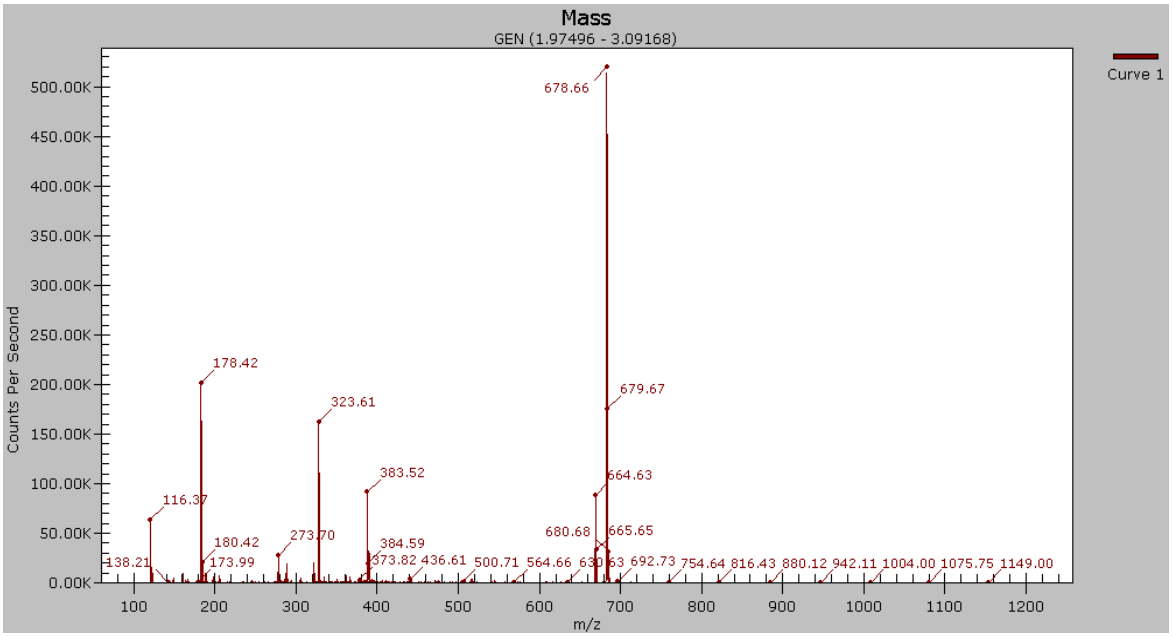

Figure S8. ESI-MS spectrum of **4** in MeCN.

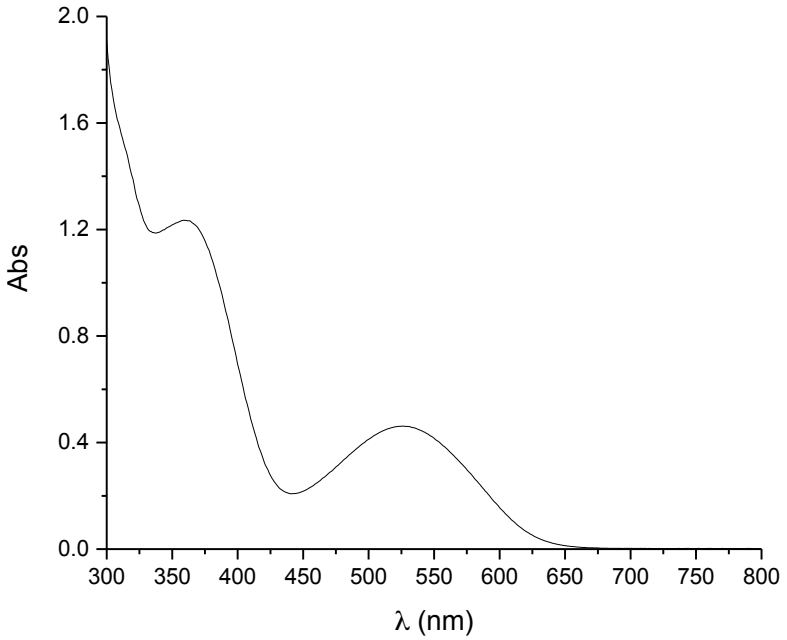

Figure S9. UV-Visible spectrum of **1** in DMSO (2.0 x 10^{-4} mol.L^{-1}).

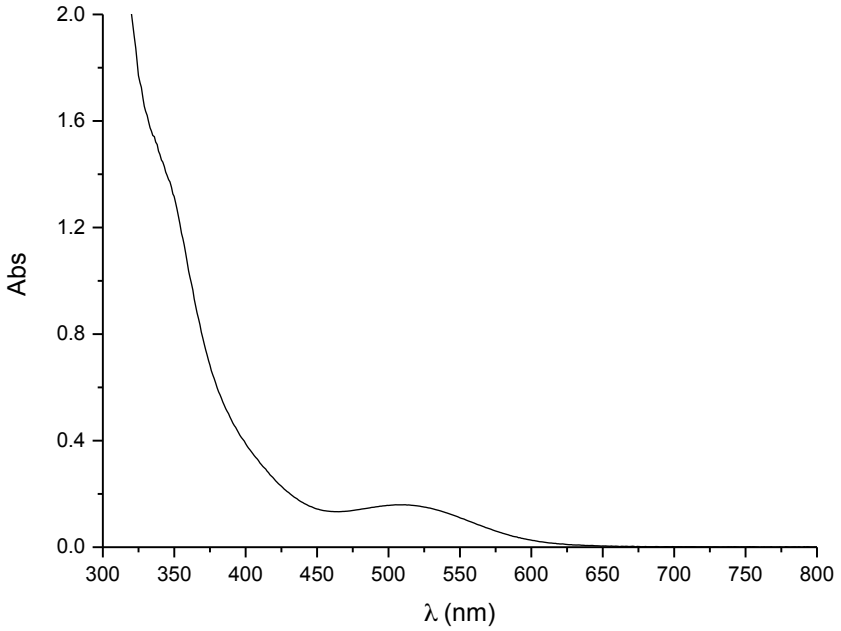

Figure S10. UV-Visible spectrum of **2** in DMSO (2.0 x 10^{-4} mol.L^{-1}).

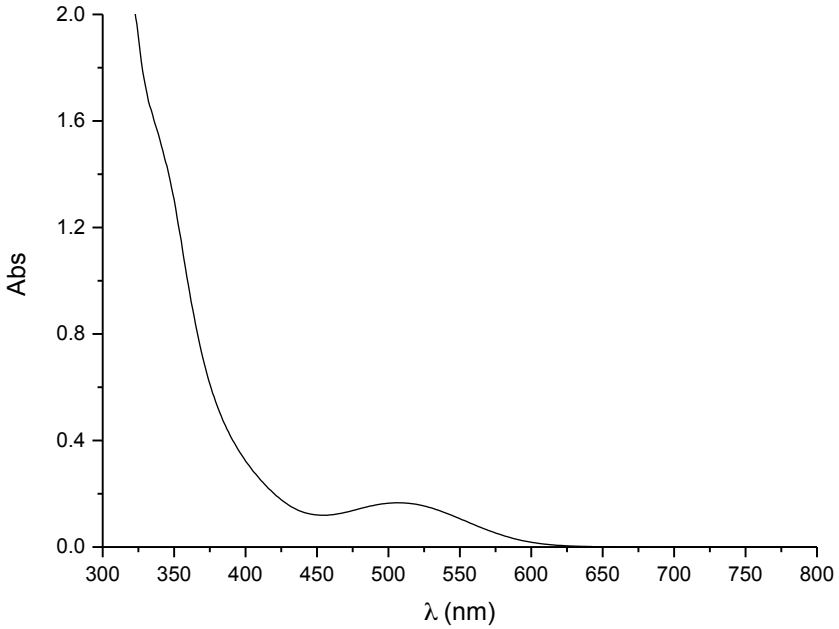

Figure S11. UV-Visible spectrum of **3** in DMSO (2.0 x 10^{-4} mol.L^{-1}).

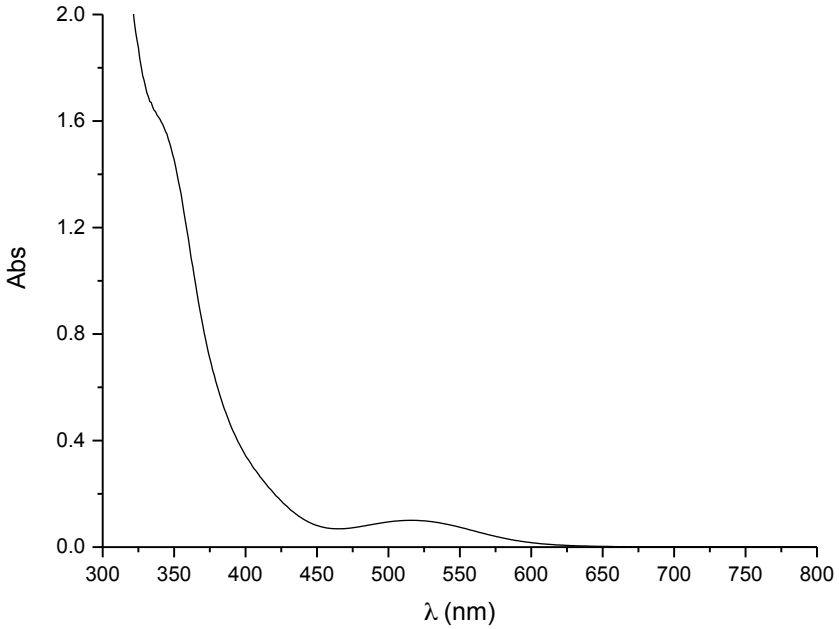

Figure S12. UV-Visible spectrum of **4** in DMSO (2.0 x 10^{-4} mol.L^{-1}).

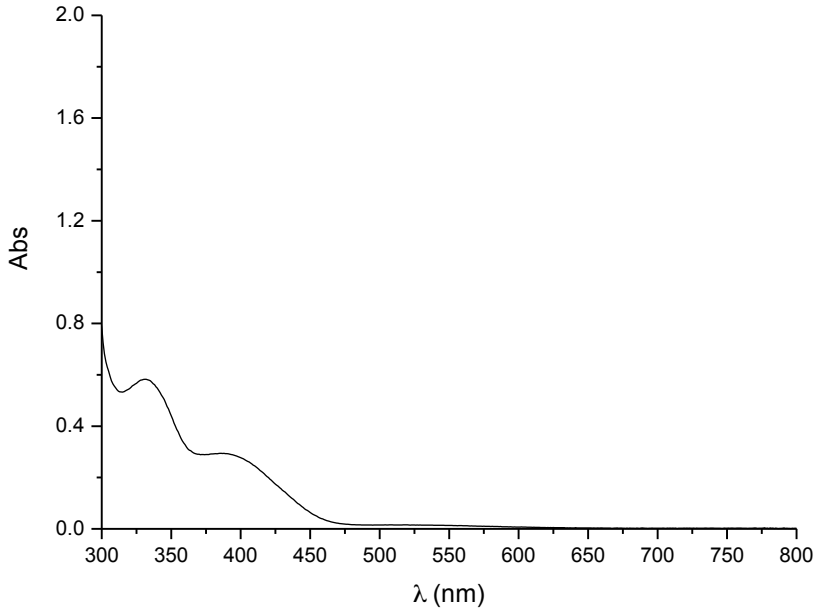

Figure S13. UV-Visible spectrum of HNQ-CH_3 in DMSO (2.0 x 10^{-4} mol.L^{-1}).

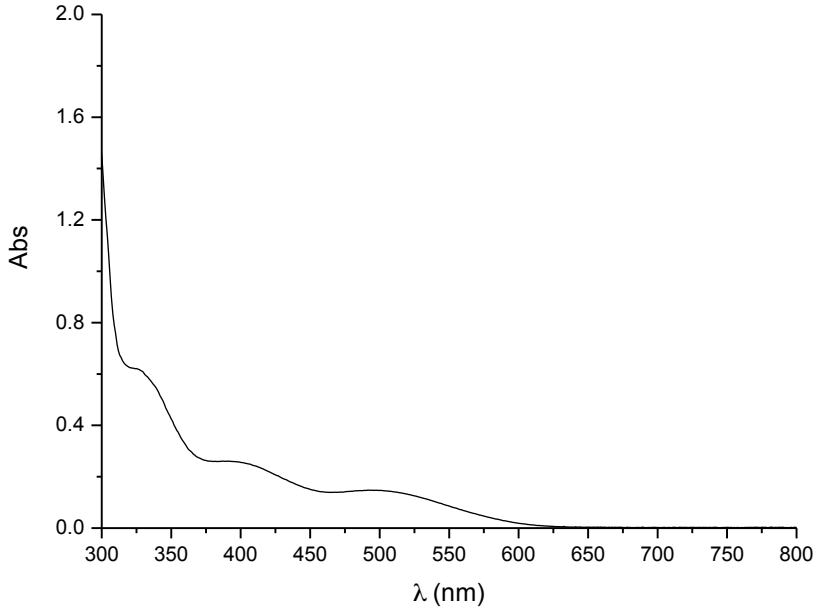

Figure S14. UV-Visible spectrum of HNQ-Cl in DMSO (2.0 x 10^{-4} mol.L^{-1}).

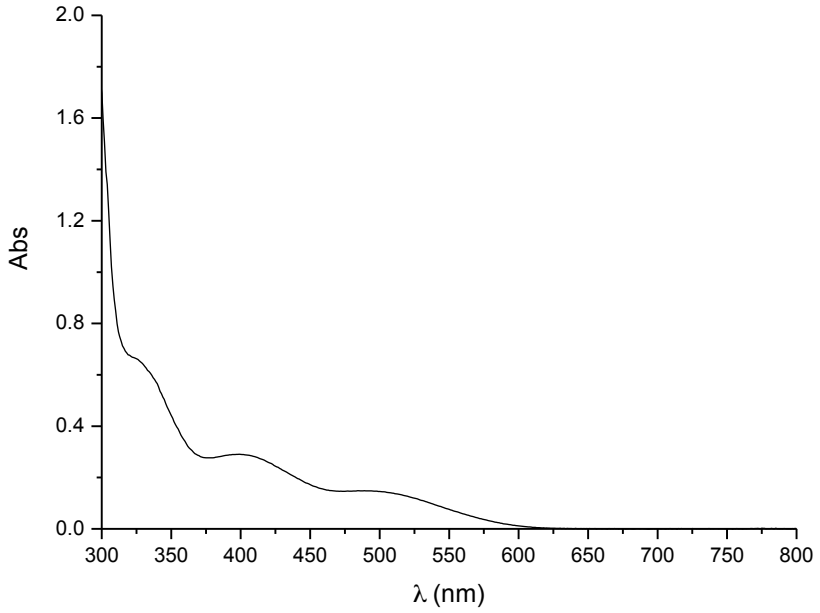

Figure S15. UV-Visible spectrum of HNQ-Br in DMSO (2.0 x 10^{-4} mol.L^{-1}).

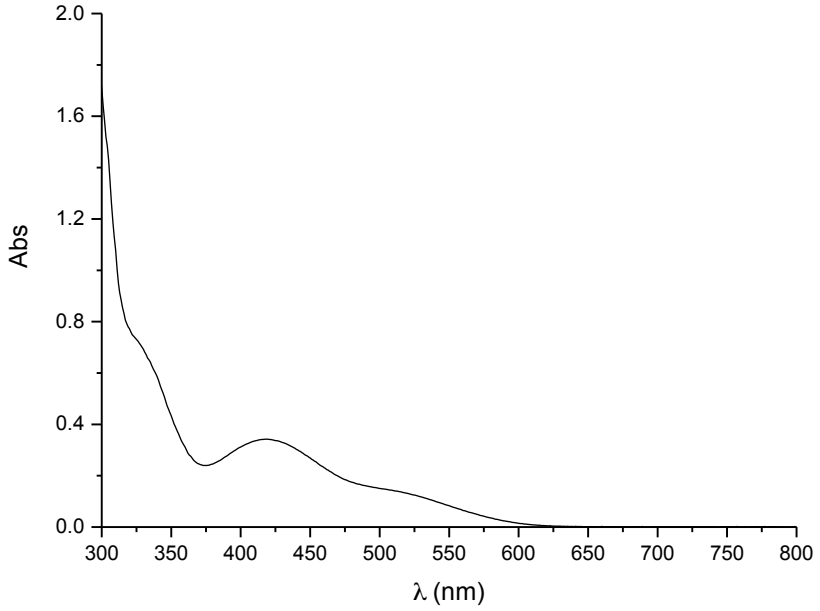

Figure S16. UV-Visible spectrum of HNQ-I in DMSO (2.0 x 10^{-4} mol.L^{-1}).

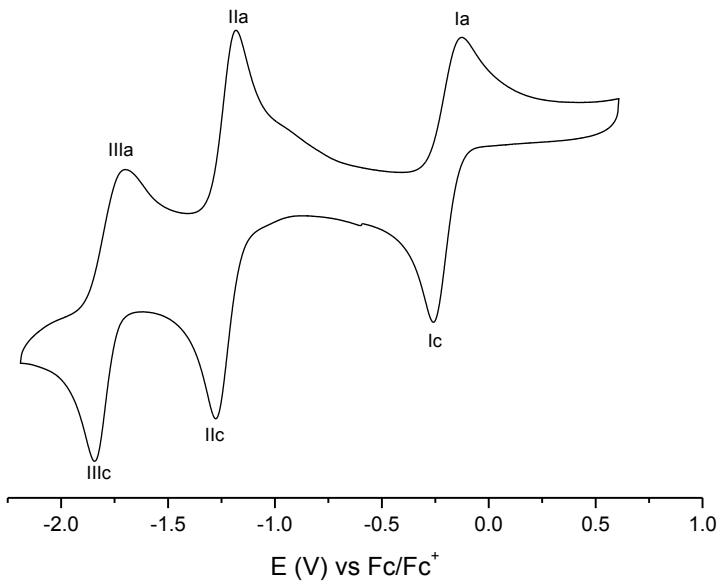

Figure S17. Cyclic voltammogram of **1** in MeCN (1 x 10^{-4} mol.L^{-1}) with $TBAClO_4$ 0.1 M, at 0.1 V/s, using a three electrode arrange (work.: carbon; ref.: Ag/AgCl (org.); aux.: Pt wire). Fc/Fc^+ was used as an internal reference.

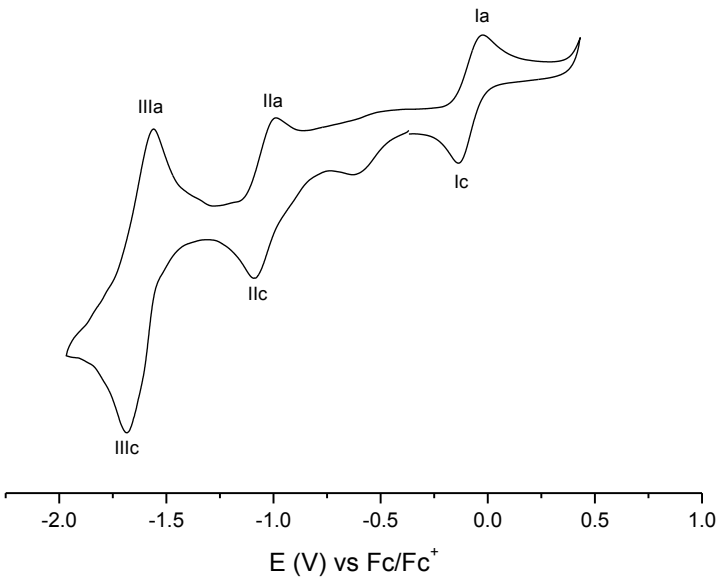

Figure S18. Cyclic voltammogram of **2** in MeCN (1 x 10^{-4} mol.L^{-1}) with $TBAClO_4$ 0.1 M, at 0.1 V/s, using a three electrode arrange (work.: carbon; ref.: Ag/AgCl (org.); aux.: Pt wire). Fc/Fc^+ was used as an internal reference.

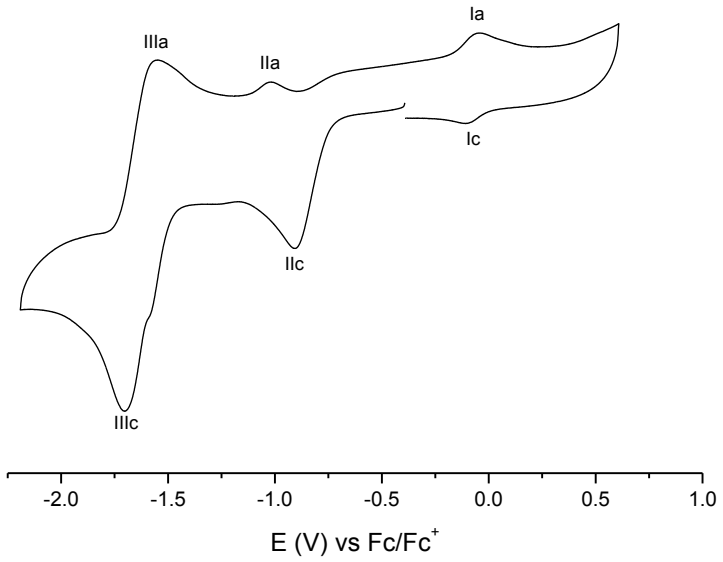

Figure S19. Cyclic voltammogram of **3** in MeCN (1 x 10^{-4} mol.L^{-1}) with $TBAClO_4$ 0.1 M, at 0.1 V/s, using a three electrode arrange (work.: carbon; ref.: Ag/AgCl (org.); aux.: Pt wire). Fc/Fc^+ was used as an internal reference.

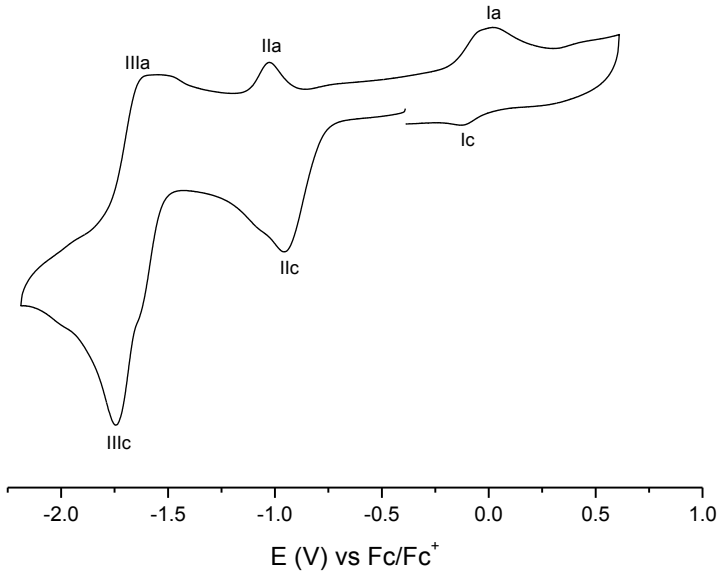

Figure S20. Cyclic voltammogram of **4** in MeCN (1 x 10^{-4} mol.L^{-1}) with $TBAClO_4$ 0.1 M, at 0.1 V/s, using a three electrode arrange (work.: carbon; ref.: Ag/AgCl (org.); aux.: Pt wire). Fc/Fc^+ was used as an internal reference.

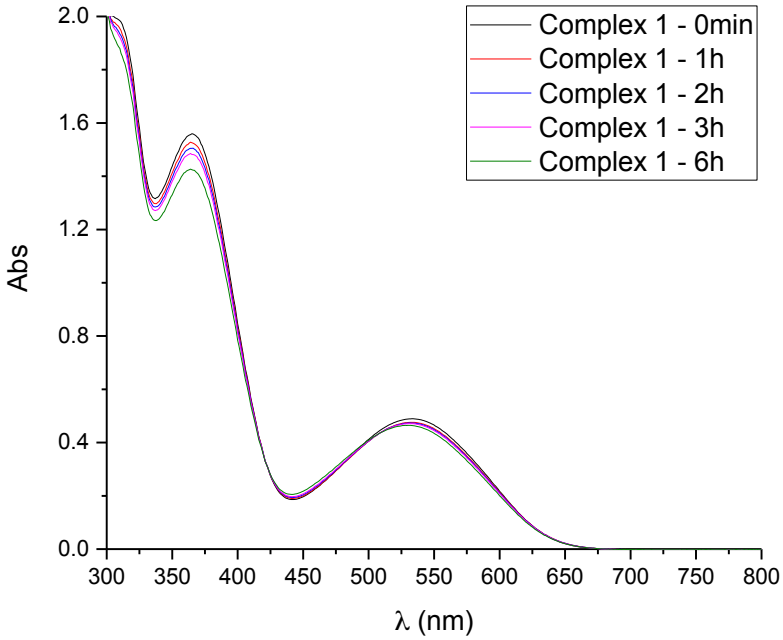

Figure S21. UV-Visible spectra of **1** (2.0 x 10^{-4} mol.L^{-1}) in DMSO/phosphate buffer 1:9 at pH 6.2, from freshly prepared solution.

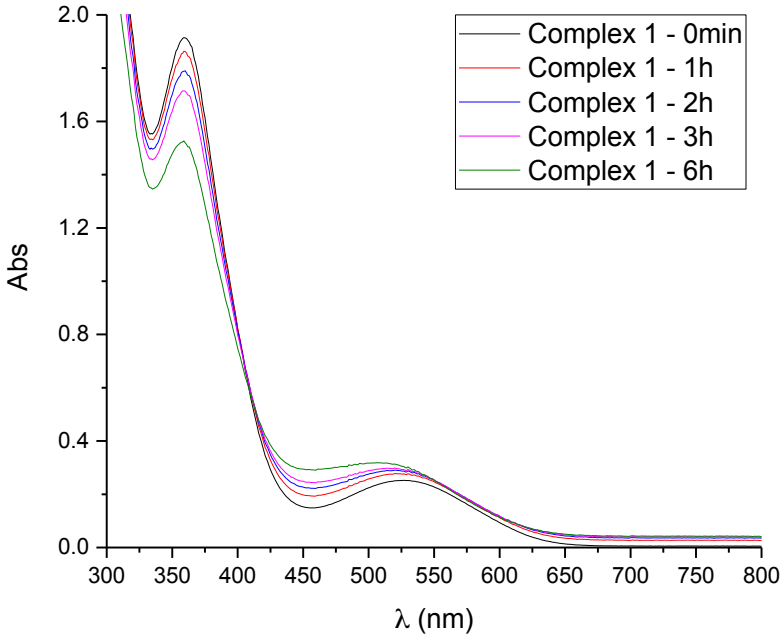

Figure S22. UV-Visible spectra of **1** (2.0 x 10^{-4} mol.L^{-1}) in DMSO/phosphate buffer 1:9 at pH 7.0, from freshly prepared solution.

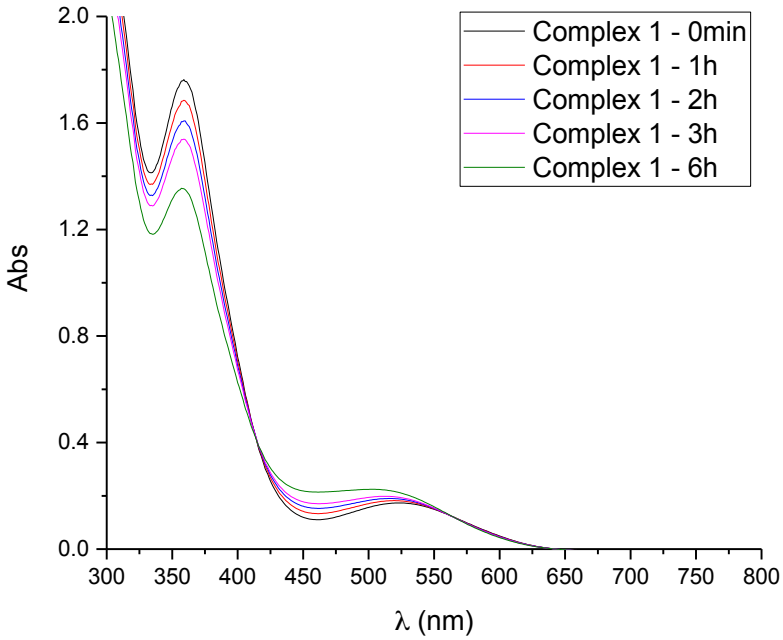

Figure S23. UV-Visible spectra of **1** (2.0 x 10^{-4} mol.L^{-1}) in DMSO/phosphate buffer 1:9 at pH 7.4, from freshly prepared solution.

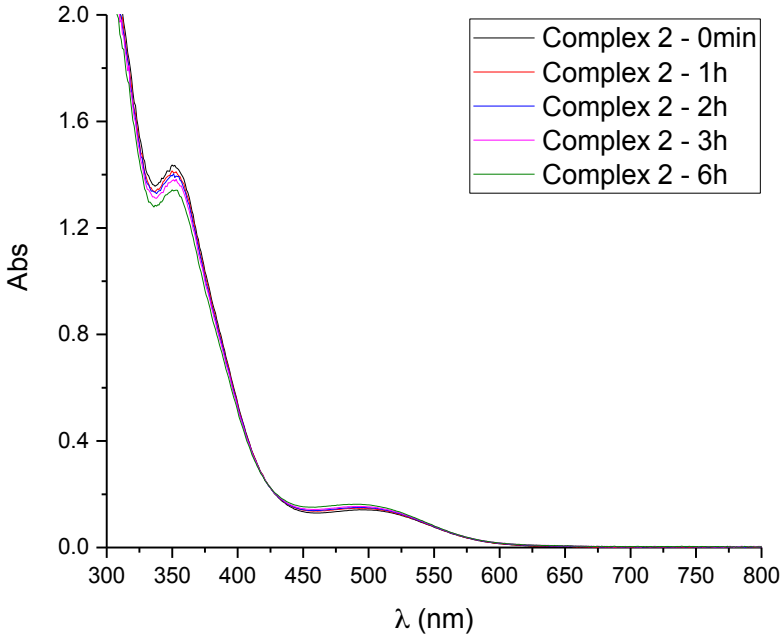

Figure S24. UV-Visible spectra of **2** (2.0 x 10^{-4} mol.L^{-1}) in DMSO/phosphate buffer 1:9 at pH 6.2, from freshly prepared solution.

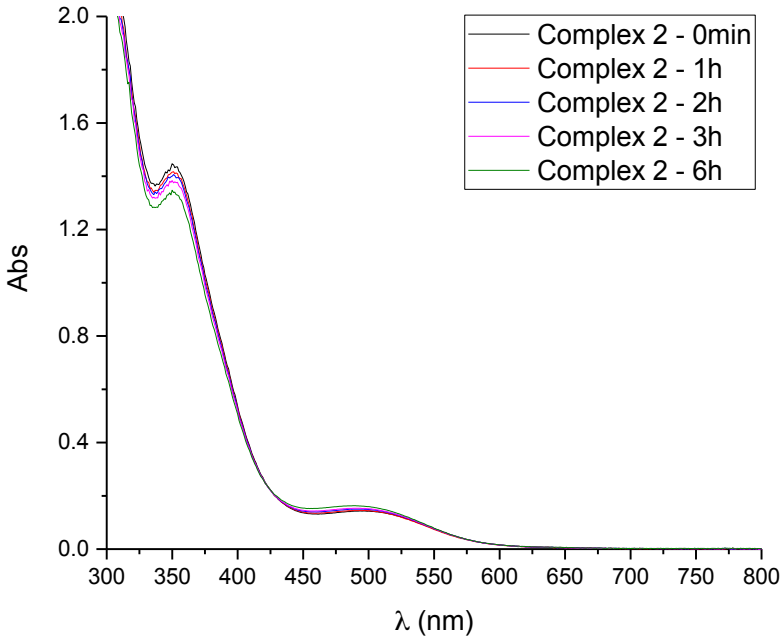

Figure S25. UV-Visible spectra of **2** (2.0 x 10^{-4} mol.L^{-1}) in DMSO/phosphate buffer 1:9 at pH 7.0, from freshly prepared solution.

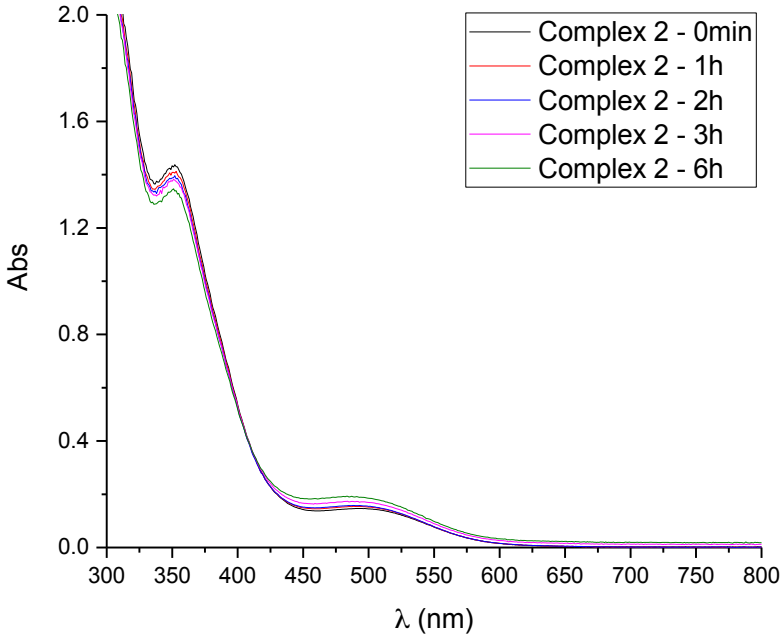

Figure S26. UV-Visible spectra of **2** (2.0 x 10^{-4} mol.L^{-1}) in DMSO/phosphate buffer 1:9 at pH 7.4, from freshly prepared solution.

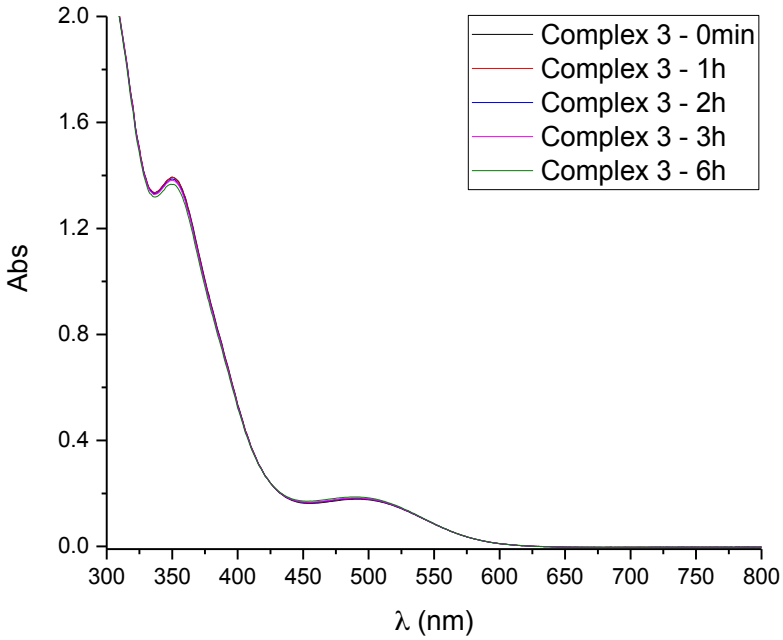

Figure S27. UV-Visible spectra of **3** (2.0 x 10^{-4} mol.L^{-1}) in DMSO/phosphate buffer 1:9 at pH 6.2, from freshly prepared solution.

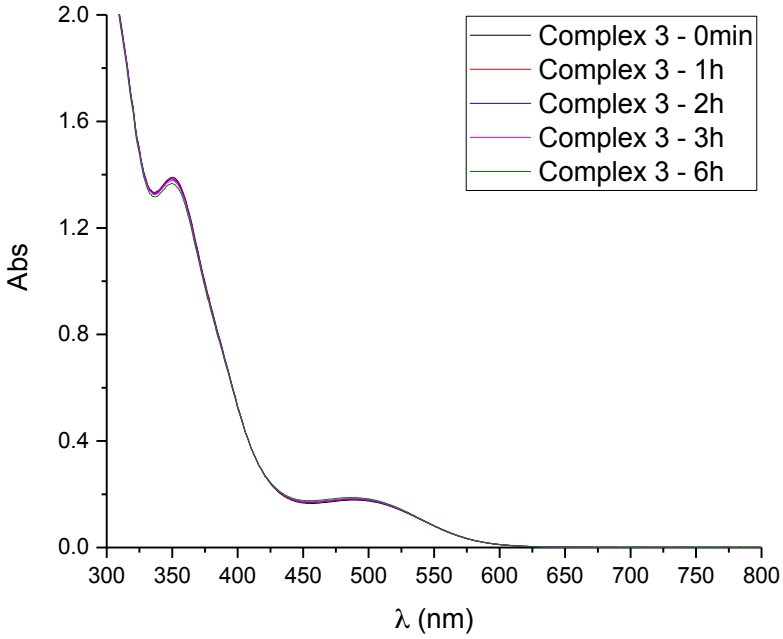

Figure S28. UV-Visible spectra of **3** (2.0 x 10^{-4} mol.L^{-1}) in DMSO/phosphate buffer 1:9 at pH 7.0, from freshly prepared solution.

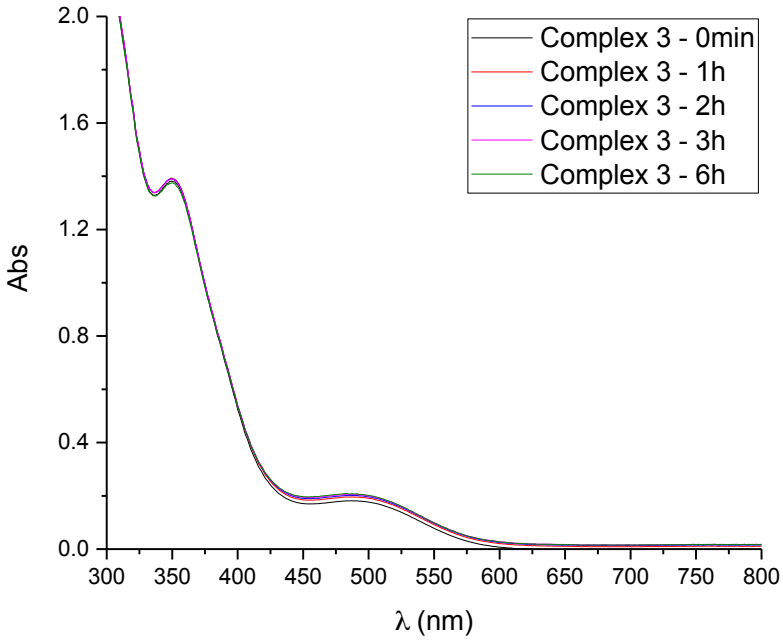

Figure S29. UV-Visible spectra of **3** (2.0 x 10^{-4} mol.L^{-1}) in DMSO/phosphate buffer 1:9 at pH 7.4, from freshly prepared solution.

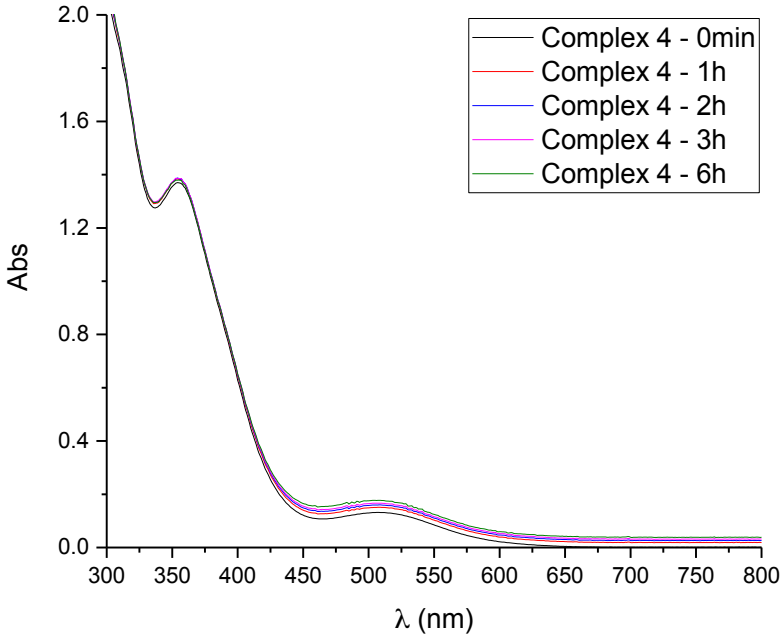

Figure S30. UV-Visible spectra of **4** (2.0 x 10^{-4} mol.L^{-1}) in DMSO/phosphate buffer 1:9 at pH 6.2, from freshly prepared solution.

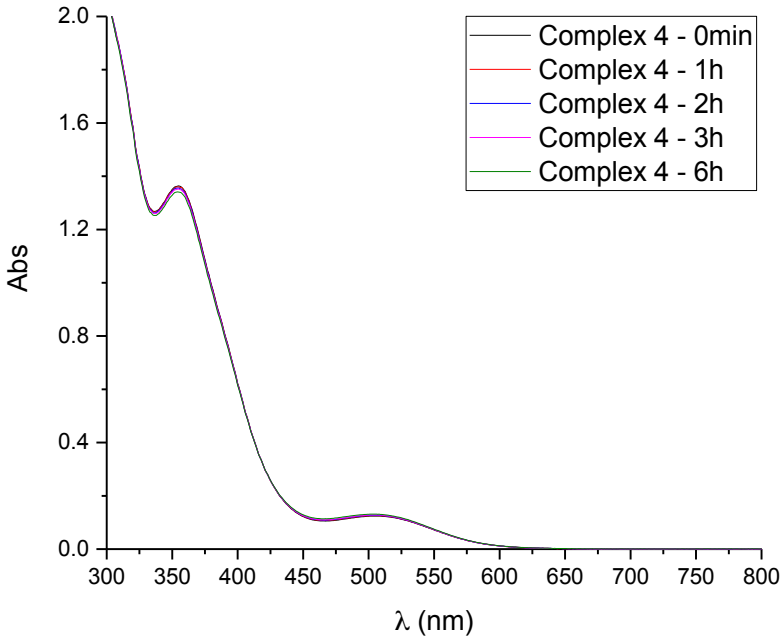

Figure S31. UV-Visible spectra of **4** (2.0 x 10^{-4} mol.L^{-1}) in DMSO/phosphate buffer 1:9 at pH 7.0, from freshly prepared solution.

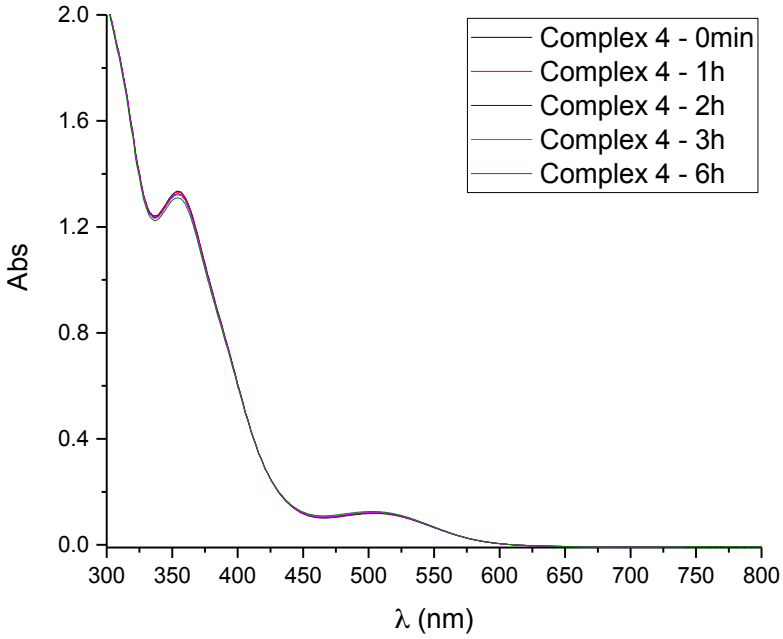

Figure S32. UV-Visible spectra of **4** (2.0 x 10^{-4} mol.L^{-1}) in DMSO/phosphate buffer 1:9 at pH 7.4, from freshly prepared solution.

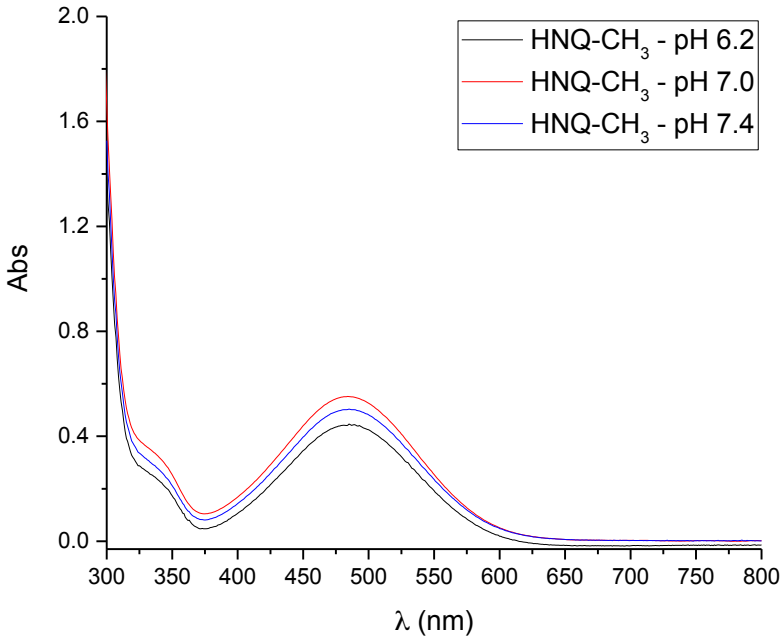

Figure S33. UV-Visible spectra of HNQ-CH_3 (2.0 x 10^{-4} mol.L^{-1}) in DMSO/phosphate buffer 1:9 at pH 6.2, 7.0 and 7.4.

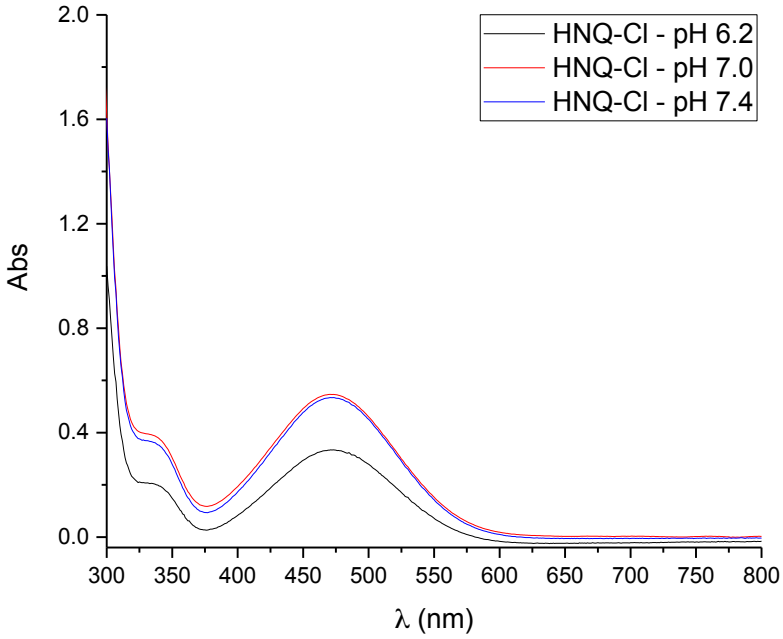

Figure S34. UV-Visible spectra of HNQ-Cl (2.0 x 10^{-4} mol.L^{-1}) in DMSO/phosphate buffer 1:9 at pH 6.2, 7.0 and 7.4.

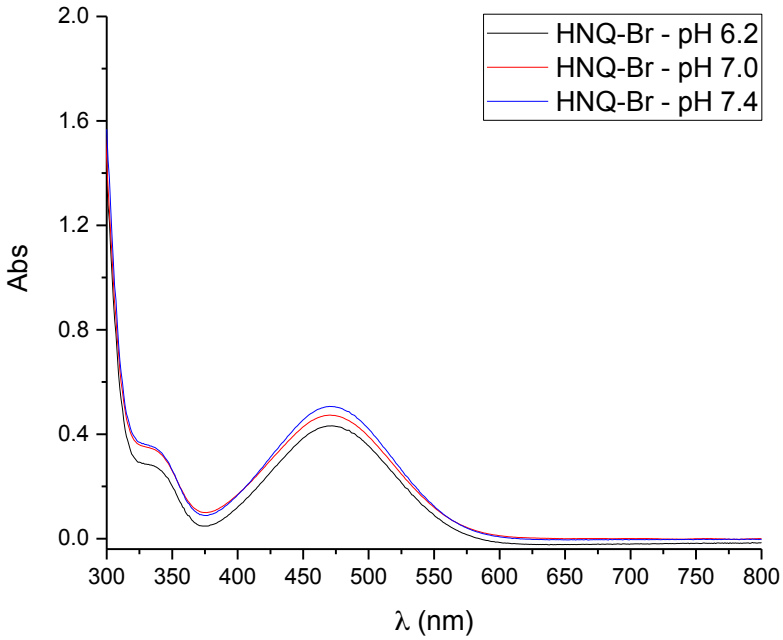

Figure S35. UV-Visible spectra of HNQ-Br (2.0 x 10^{-4} mol.L^{-1}) in DMSO/phosphate buffer 1:9 at pH 6.2, 7.0 and 7.4.

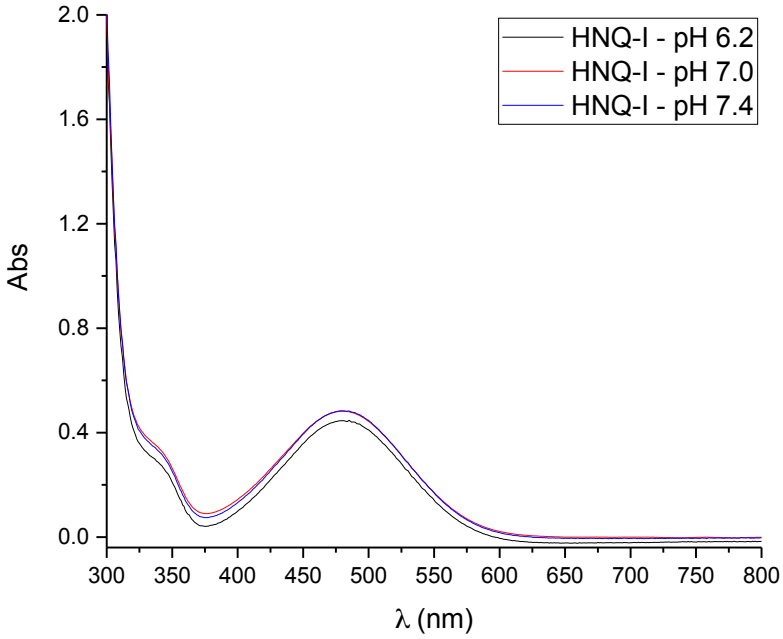

Figure S36. UV-Visible spectra of HNQ-I (2.0 x 10^{-4} mol.L^{-1}) in DMSO/phosphate buffer 1:9 at pH 6.2, 7.0 and 7.4.

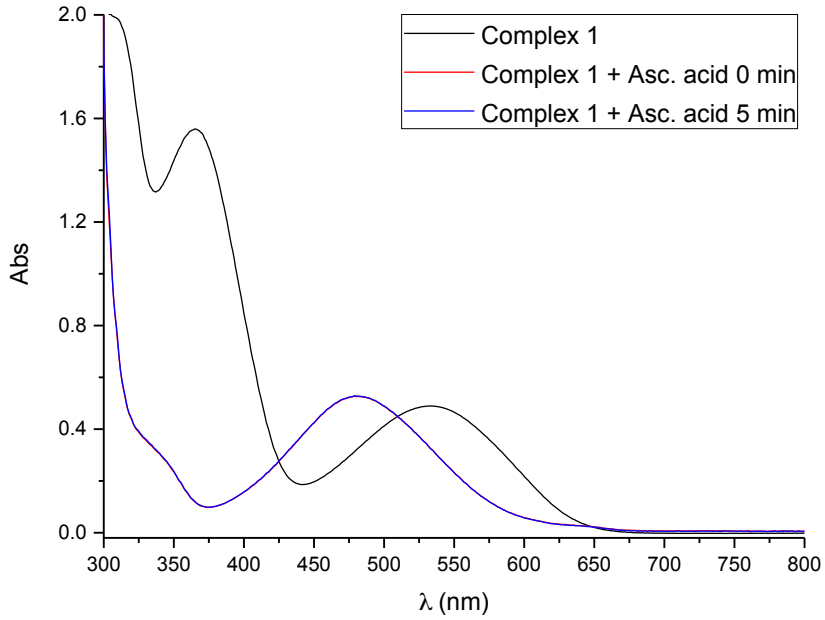

Figure S37. UV-Visible spectra of **1** (2.0 x 10^{-4} mol.L^{-1}) in DMSO/phosphate buffer 1:9 at pH 6.2 and in the presence of ten equivalents of ascorbic acid (AA) (2.0 x 10^{-3} mol.L^{-1}).

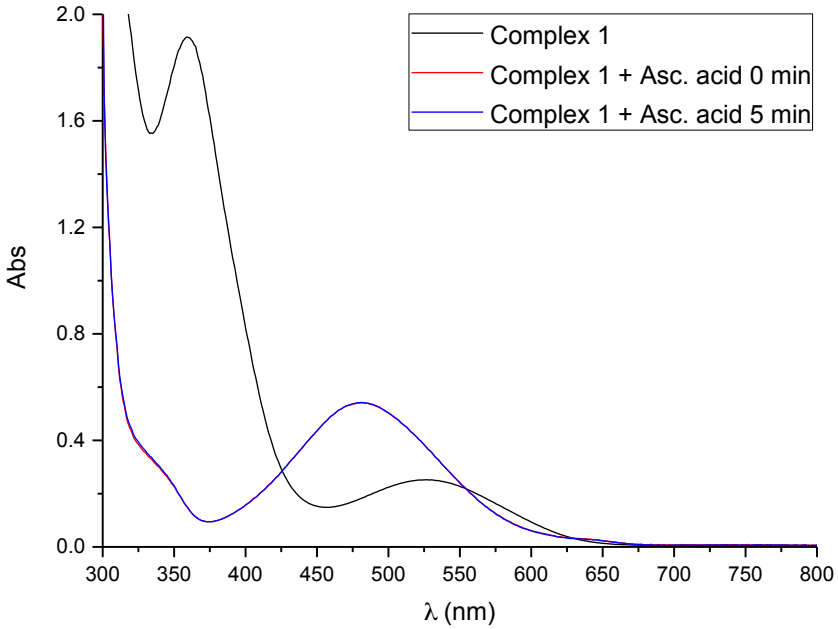

Figure S38. UV-Visible spectra of **1** (2.0 x 10^{-4} mol.L^{-1}) in DMSO/phosphate buffer 1:9 at pH 7.0 and in the presence of ten equivalents of ascorbic acid (AA) (2.0 x 10^{-3} mol.L^{-1}).

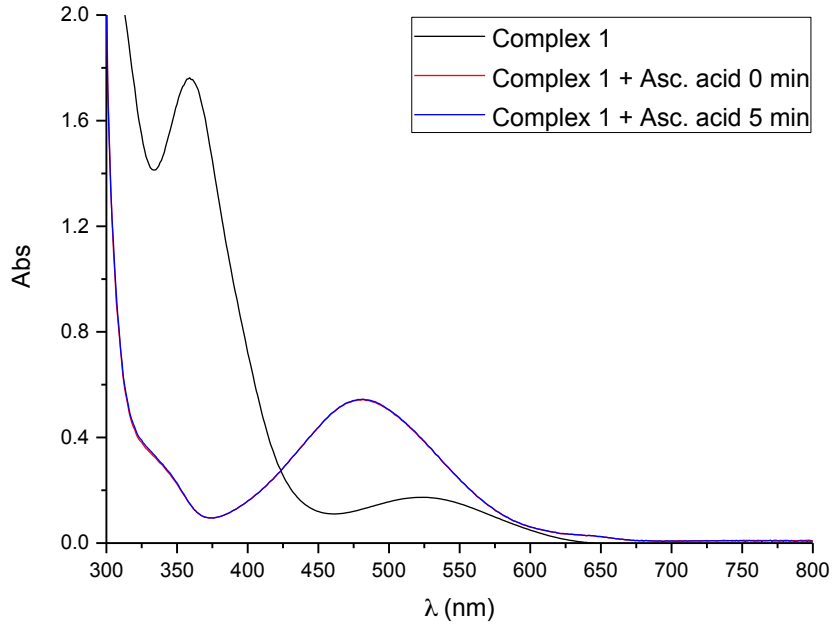

Figure S39. UV-Visible spectra of **1** (2.0 x 10^{-4} mol.L^{-1}) in DMSO/phosphate buffer 1:9 at pH 7.4 and in the presence of ten equivalents of ascorbic acid (AA) (2.0 x 10^{-3} mol.L^{-1}).

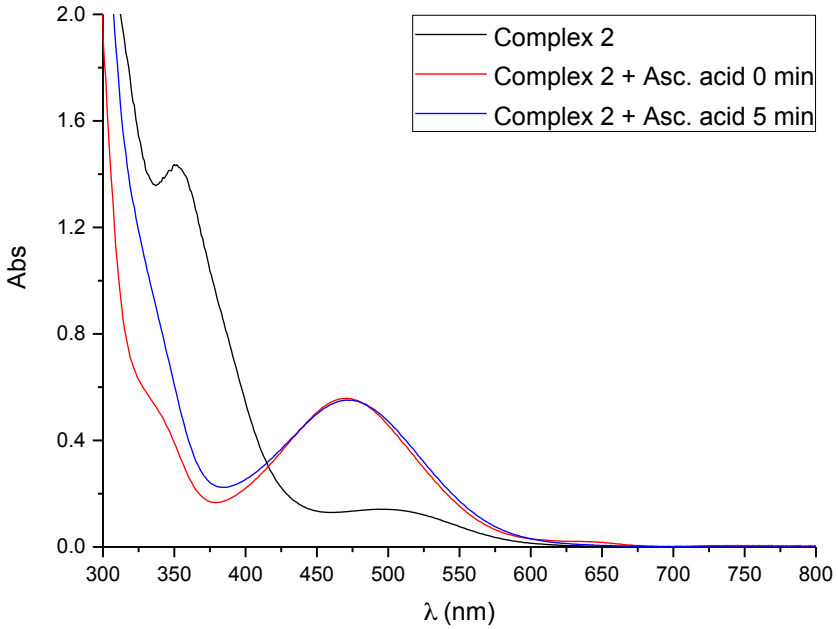

Figure S40. UV-Visible spectra of **2** (2.0 x 10^{-4} mol.L^{-1}) in DMSO/phosphate buffer 1:9 at pH 6.2 and in the presence of ten equivalents of ascorbic acid (AA) (2.0 x 10^{-3} mol.L^{-1}).

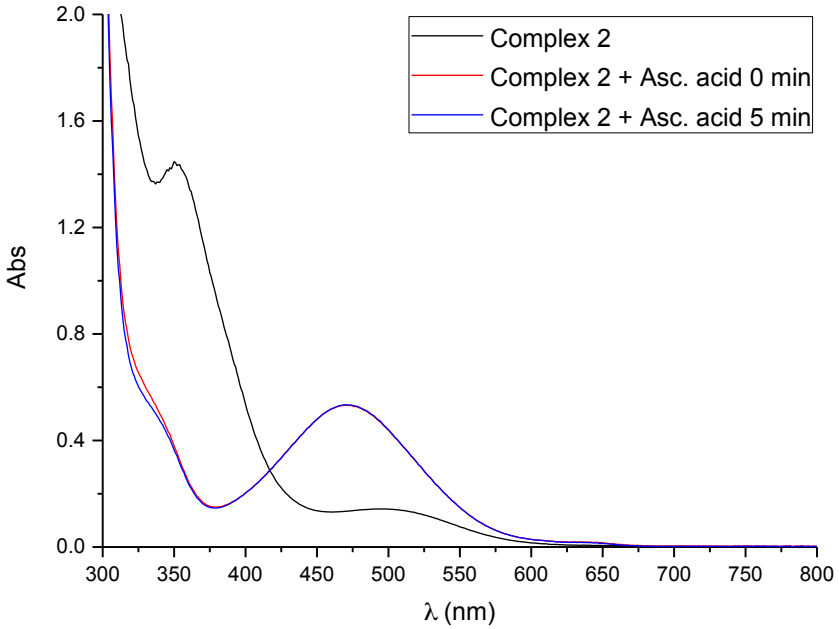

Figure S41. UV-Visible spectra of **2** (2.0 x 10^{-4} mol.L^{-1}) in DMSO/phosphate buffer 1:9 at pH 7.0 and in the presence of ten equivalents of ascorbic acid (AA) (2.0 x 10^{-3} mol.L^{-1}).

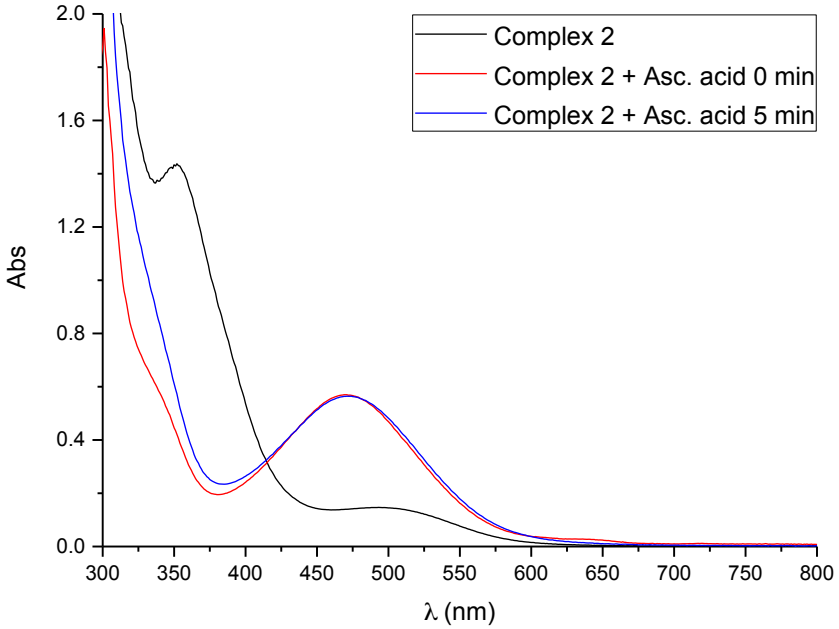

Figure S42. UV-Visible spectra of **2** (2.0 x 10^{-4} mol.L^{-1}) in DMSO/phosphate buffer 1:9 at pH 7.4 and in the presence of ten equivalents of ascorbic acid (AA) (2.0 x 10^{-3} mol.L^{-1}).

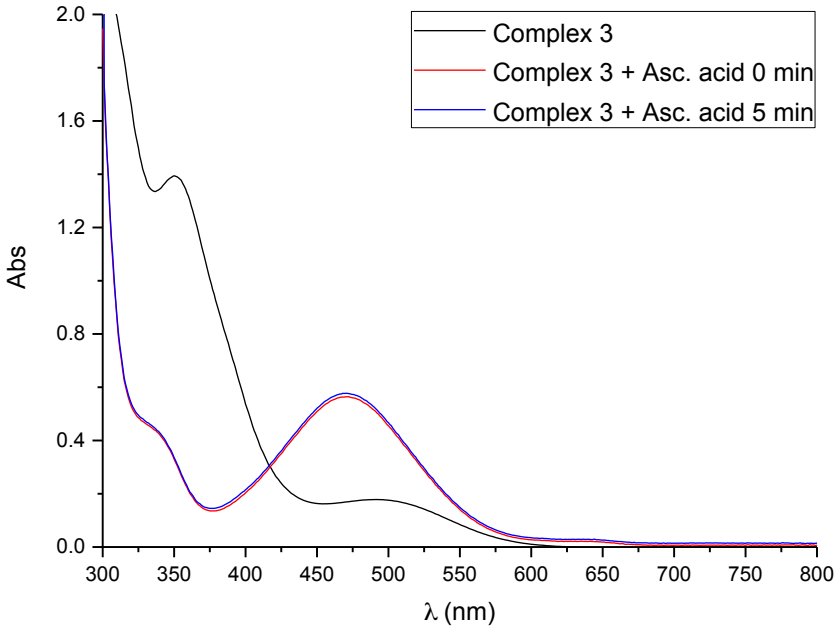

Figure S43. UV-Visible spectra of **3** (2.0 x 10^{-4} mol.L^{-1}) in DMSO/phosphate buffer 1:9 at pH 6.2 and in the presence of ten equivalents of ascorbic acid (AA) (2.0 x 10^{-3} mol.L^{-1}).

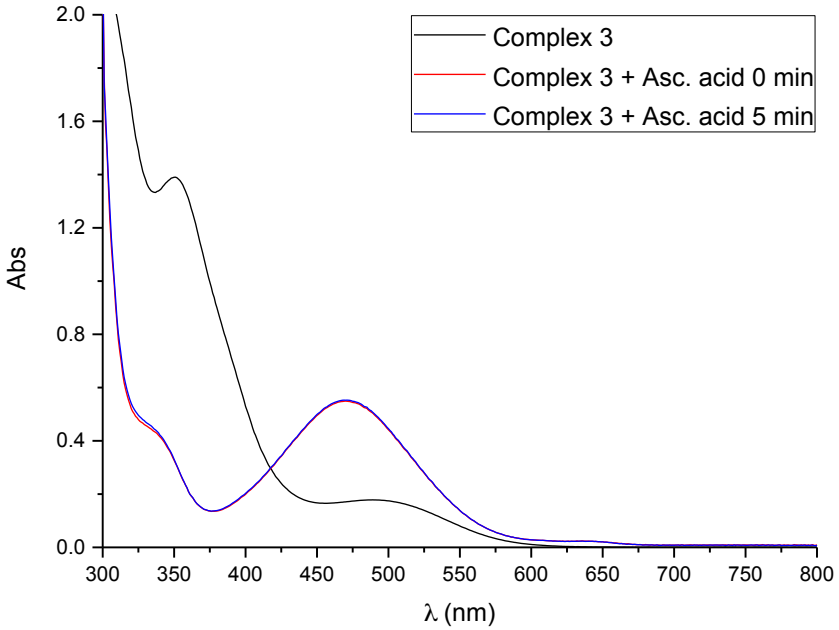

Figure S44. UV-Visible spectra of **3** (2.0 x 10^{-4} mol.L^{-1}) in DMSO/phosphate buffer 1:9 at pH 7.0 and in the presence of ten equivalents of ascorbic acid (AA) (2.0 x 10^{-3} mol.L^{-1}).

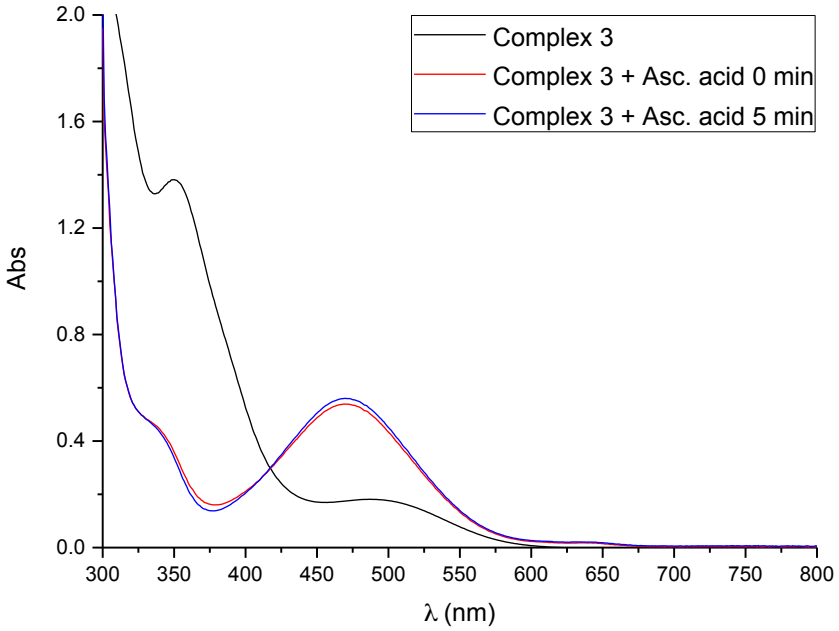

Figure S45. UV-Visible spectra of **3** (2.0 x 10^{-4} mol.L^{-1}) in DMSO/phosphate buffer 1:9 at pH 7.4 and in the presence of ten equivalents of ascorbic acid (AA) (2.0 x 10^{-3} mol.L^{-1}).

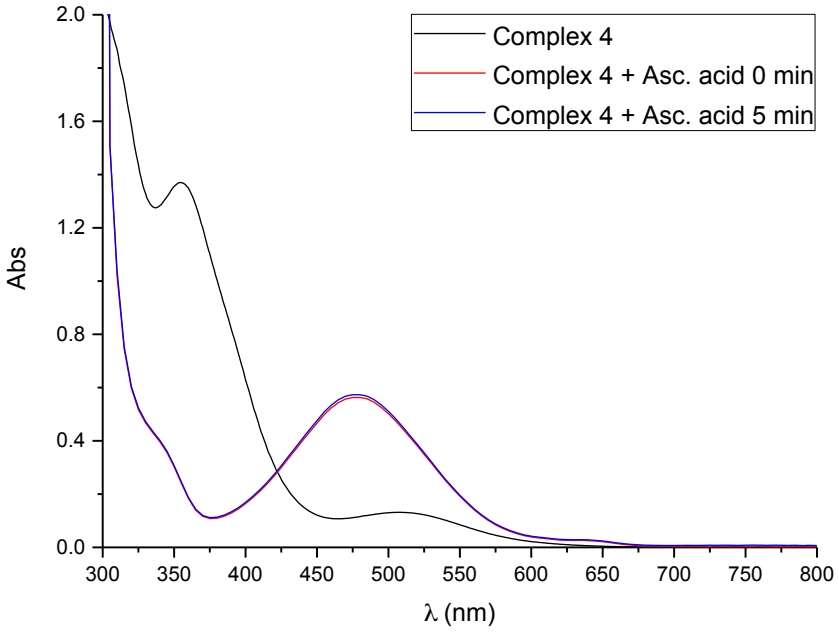

Figure S46. UV-Visible spectra of **4** (2.0 x 10^{-4} mol.L^{-1}) in DMSO/phosphate buffer 1:9 at pH 6.2 and in the presence of ten equivalents of ascorbic acid (AA) (2.0 x 10^{-3} mol.L^{-1}).

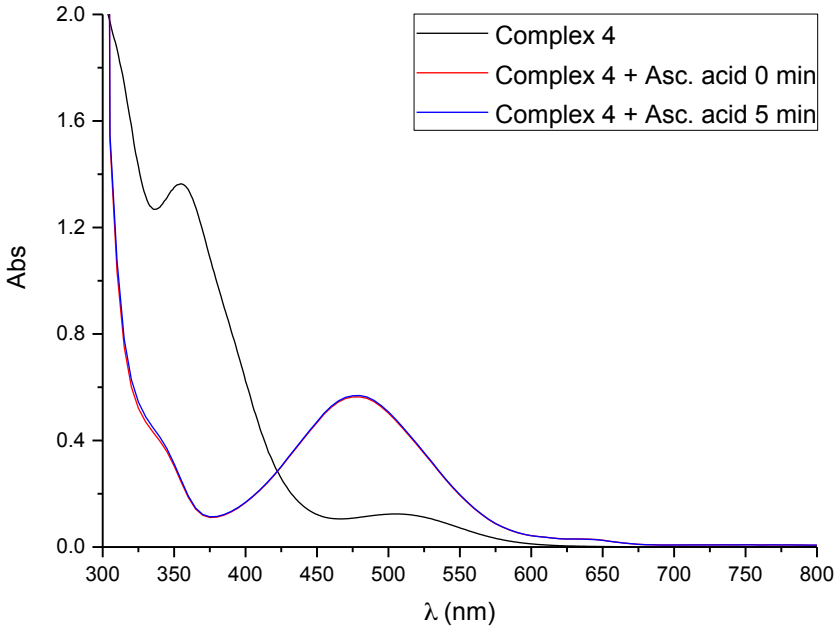

Figure S47. UV-Visible spectra of **4** (2.0 x 10^{-4} mol.L^{-1}) in DMSO/phosphate buffer 1:9 at pH 7.0 and in the presence of ten equivalents of ascorbic acid (AA) (2.0 x 10^{-3} mol.L^{-1}).

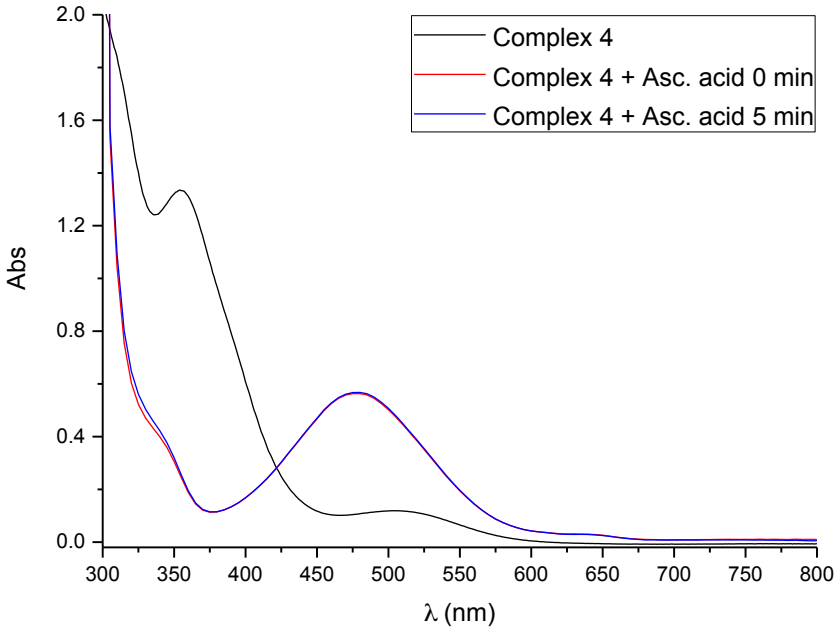

Figure S48. UV-Visible spectra of **4** (2.0 x 10^{-4} mol.L^{-1}) in DMSO/phosphate buffer 1:9 at pH 7.4 and in the presence of ten equivalents of ascorbic acid (AA) (2.0 x 10^{-3} mol.L^{-1}).

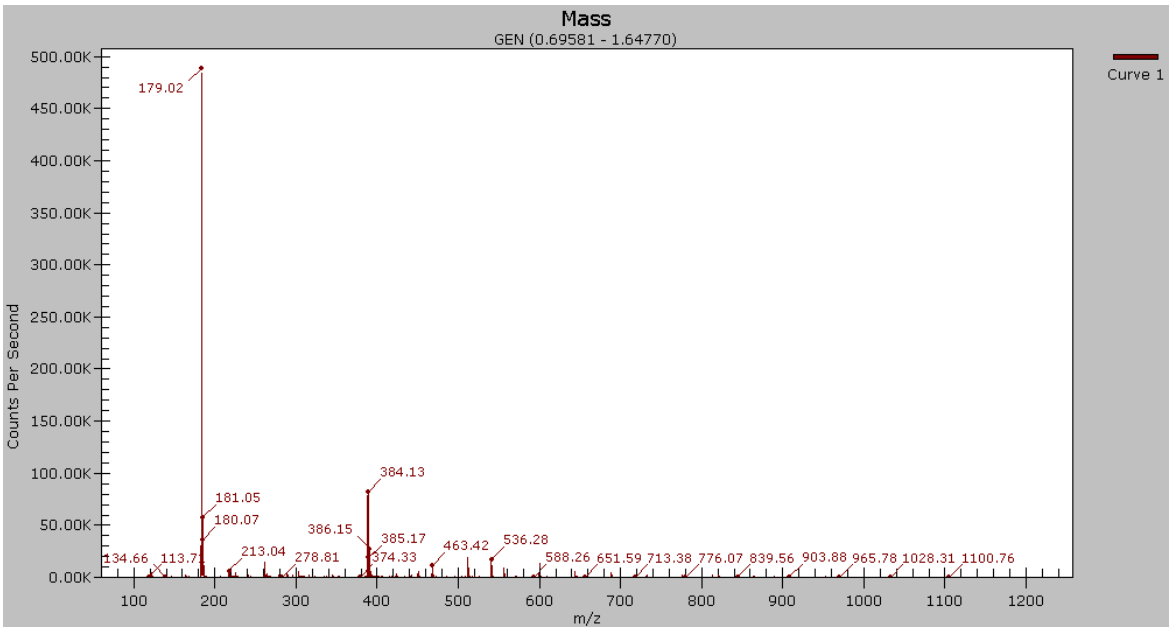

Figure S49. ESI-MS (positive scan) spectrum of **1** after reaction with ascorbic acid.

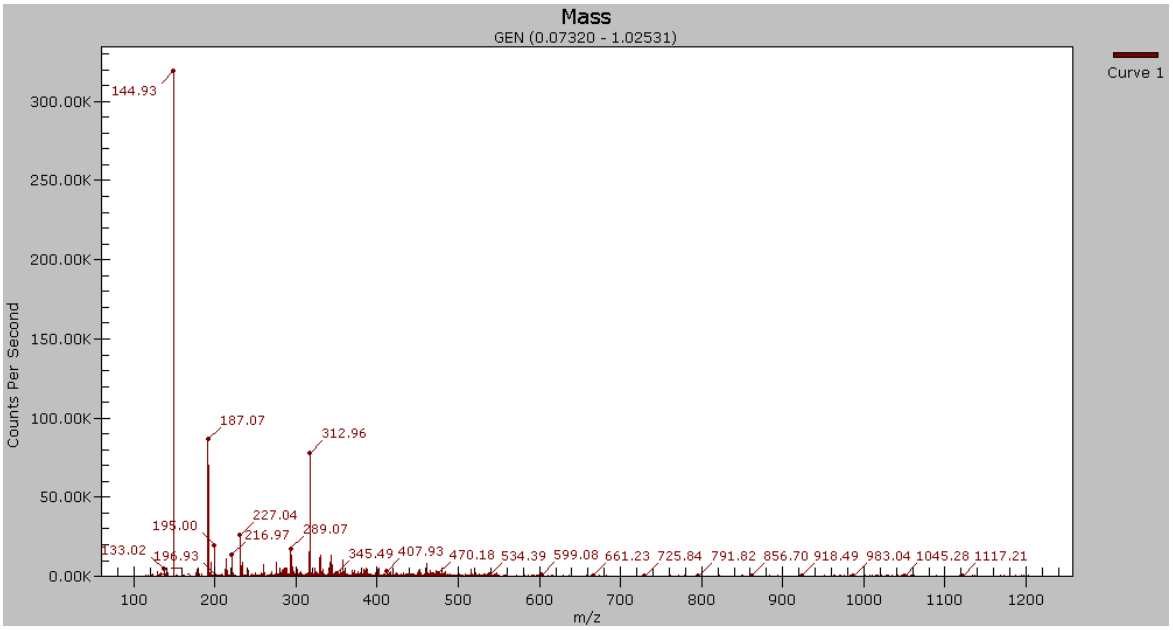

Figure S50. ESI-MS (negative scan) spectrum of **1** after reaction with ascorbic acid.